Heteropolyacid (H$_3$PW$_{12}$O$_{40}$) supported MCM-41: An efficient solid acid catalyst for the green synthesis of xanthenedione derivatives

G. Karthikeyan [a], A. Pandurangan [a,b,*]

[a] Department of Chemistry, Anna University, Guindy, Chennai 600 025, India
[b] Institute of Catalysis and Petroleum Technology, A. C. Tech Campus, Anna University Chennai, Chennai 600 025, India

ARTICLE INFO

ABSTRACT

HPWA/MCM-41 mesoporous molecular sieves of appropriate ratios were prepared by loading HPWA on siliceous MCM-41 by the wet impregnation method. The prepared HPWA/MCM-41 materials were characterized by X-ray diffraction analysis (XRD) and BET surface area and FT-IR measurements. The morphology of mesoporous materials was studied by TEM observation. The catalytic activity of the above materials was tested for the condensation of dimedone (active methylene carbonyl compound) and various aromatic aldehyes under liquid phase conditions at 90 °C. The products were confirmed by FT-IR, ^{1}H NMR and ^{13}C NMR studies. HPWA supported MCM-41 catalysts catalyses efficiently the condensation of dimedone and aromatic aldehydes in ethanol and other solvents under liquid phase conditions to afford the corresponding xanthenedione derivatives. Activities of the catalysts follow the order: HPWA/MCM-41(20 wt.%) > HPWA/MCM-41(30 wt.%) > H$_3$PW$_{12}$O$_{40}$·nH$_2$O > HPWA/MCM-41(10 wt.%) > HPWA/SiO$_2$ (20 wt.%) > HM (12) > Hβ (8) > Al-MCM-41 (50). Various advantages associated with these protocols include simple workup procedure, short reaction times, high product yields and easy recovery and reusability of the catalyst.

© 2009 Elsevier B.V. All rights reserved.

1. Introduction

Xanthene derivatives are indispensable in the field of medicinal chemistry for their biologically active properties as they have been synthesised and evaluated for their potential as anti-depressants and antimalarial [1]. Among them, xanthenediones forms the structural unit in many of the natural product compounds [2,3] and are used as versatile synthons for their inherent reactivity [4] due to the presence of inbuilt pyran ring. It was our interest to synthesis xanthenediones, since it possess a potential antimicrobial activity [5] similar to ampicilin and chlotrimazole, against *Staphlococcus aureus* and *Candida albicans*, respectively. Xanthenediones are synthesised by many procedures in recent years and one among the conventional methods involve acid- or base-catalyzed condensation of appropriate active methylene carbonyl compounds with aldehydes [6], since the active methylene compounds like dimedone is used as a precursor for many heterocyclic compounds [7–9]. The formation of xanthenediones usually condenses active methylene carbonyl compounds with aldehydes catalyzed by sulfuric acid or hydrochloric acid [10] and many methods for the synthesis has

been adopted [11,12]. Many authors attempted to use solid acid catalysts and ionic liquids as catalysts to synthesise xanthenediones. InCl$_3$·4H$_2$O catalyzed reaction has been reported for the preparation of xanthenedione derivatives in ionic liquids [13]. Recently, the synthesis of xanthenedione derivatives has been reported through condensation reactions between aromatic aldehydes and dimedone using Fe^{3+}-montmorillonite as a solid acid catalyst [14] and also the synthesis of 1,8-dioxo-octahydroxanthenes (xanthenediones) over amberlyst-15 catalyst [15], FeCl3·6H$_2$O and [bmim][BF$_4$] ionic liquid [16] has been proposed. Jin et al. reported the novel procedure to synthesise xanthenediones over dodecylbenzene sulphonic acid [17]. 14-Substituted-14-H-dibenzo xanthene derivatives over HPA/SiO$_2$ [18] and Preyssler type heteropoly acid [19] has been reported recently. The synthesis of 1,8-dioxooctahydroxanthenes using tetrabutylammonium hydrogen sulphate has been performed in recent years [20]. In view of environmental aspects, heterogenous catalysts are preferable to homogenous catalysts and mineral acids such as HCl, H$_2$SO$_4$, BF$_3$, FeCl$_3$, pTSA, etc., for their green environmental character. Heterogenous solid acid catalysts are important in catalysis field for their easy synthesis procedures, recoverability and reusability, referred to as environmentally benign catalysts for their non-polluting properties. Catalysts like zeolites [21], Amberlyst-15 [22], and montmorillonite K10 clay [23] has been used for the synthesis of fine chemicals in particular. These catalysts suffer from microporosity, small surface area and complicated intermediate steps rendering the main product such that the

* Corresponding author at: Department of Chemistry, Anna University, CEG, Sardhar Patel Road, Guindy, Chennai 600 025, Tamil Nadu, India. Tel.: +91 44 22203158; fax: +91 44 22200660.

E-mail address: pandurangan_a@yahoo.com (A. Pandurangan).

larger organic molecules cannot pass through their pores resulting in the limited selectivity and conversion. In recent years, many researchers reported that the MCM-41 type heterogenous catalysts favours alkylation and acylation reactions [24–26], acetalyzation [27], rearrangements [28], esterification [29] reactions, condensation reactions [30], etc.

HPWA [31,32], HPWA supported Si-MCM-41 [33–36] and other heterogenous supported HPW catalysts [37] finds its place in catalysis over many organic reactions owing to the typical characteristics of the mesoporous materials of the MCM-41 type with highly ordered mesoporosity, large surface area, and high hydrothermal stability and acidity, alluding to the possibility of applying these materials as catalysts in the synthesis and conversion of large organic molecules. These reports paved the way for the present work as this is the first time we are reporting HPWA/MCM-41 mesoporous molecular sieves for the condensation reaction of dimedone and aromatic aldehydes to afford biologically active 1,8-dioxooctahydroxanthenes (xanthenediones) in high yields which involves simple workup procedure, short reaction times; the used green solid acid HPWA/MCM-41 type catalysts are recovered and reused.

2. Experimental

2.1. Materials

The syntheses of HPWA/MCM-41 materials were carried out by a hydrothermal method using sodium metasilicate ($Na_2SiO_3 \cdot 5H_2O$), $H_3PW_{12}O_{40} \cdot nH_2O$, cetyltrimethylammonium bromide ($C_{16}H_{33}(CH_3)_2N^+Br^-$), and sulfuric acid ($H_2SO_4$). The AR grade chemicals used were purchased from Merck. The commercial catalysts such as $H_3PW_{12}O_{40} \cdot nH_2O$, HM (12) (Si/Al = 12, PQ) and Hβ (8) (Si/Al = 8, PQ) were obtained from Sud Chemie India Ltd. Various aromatic aldehydes and 5,5-dimethyl-1,3-cyclohexanedione (dimedone) were purchased from Aldrich & Co., USA and absolute alcohol was purchased from Heymen, England and were used without further purification.

2.2. Synthesis of Si-MCM-41

Si-MCM-41 samples were synthesised hydrothermally using a gel composition of SiO_2: 0.2CTAB: $0.89H_2SO_4$: $120H_2O$ [38]. Sodium metasilicate and aluminium sulphate were used as the sources for silicon and aluminium, respectively. Cetyltrimethylammonium bromide (CTAB) was used as the template. In typical synthesis, 10.6 g of sodium metasilicate was dissolved in an appropriate amount of distilled water and stirred. The pH of the solution was adjusted to 10.5 by adding 1 M H_2SO_4 with constant stirring to form a gel. After 30 min, an aqueous solution of CTAB was added to it and the mixture was stirred for 1 h at room temperature. The suspension was then transferred into a 300 ml stainless steel autoclave, sealed and heated in a hot air oven at 145 °C for 48 h. After cooling to room temperature, the product formed was filtered, washed with deionised water and dried. The dried materials were calcined at 550 °C for 1 h in nitrogen atmosphere and for 5 h in air.

2.3. Preparation of HPWA/MCM-41 catalysts

Initially, 1 g of predried Si-MCM-41 was dispersed in 10 ml deionized water and stirred. A desired amount of HPWA (e.g. 0.1 g for 10 wt.%) is weighed and dissolved in 20 ml deionized water and this solution was added slowly to prepare the impregnated catalysts by stirring for 6 h. The residue was filtered and gently washed with deionized water in order to remove metal ions adsorbed on the external surface. The filtrate was dried under reduced pressure, and finally calcined in air at 300 °C for 5 h.

2.4. Catalytic experiments

In a general procedure, 5,5-di-methyl-1,3-cyclohexanedione (2.00 mmol), aromatic aldehyde (1.00 mmol) and catalyst (HPWA/MCM-41) 0.25 g in the presence of ethanol (5-ml) were placed in a 25 ml round-bottomed glass reactor containing magnetic stirrer and fitted with reflux condenser. The reactor was heated to 90 °C and maintained in oil bath for appropriate time. The completion of the reaction was monitored by TLC. After completion of the reaction, the solution was filtered to remove the catalyst and the clear solution (filtrate) is poured in 50 ml water in a beaker. The resulting precipitate is settled down, filtered and dried. Pure product is obtained by re-crystallization in ethanol.

All the products were characterized by ^1H NMR, ^{13}C NMR and IR and have been identified by the comparison of the spectral data with those reported. All yields refer to isolated products. NMR spectra were recorded on a Bruker 500 MHz spectrometer. IR spectra were run on a PerkinElmer bio-spectrometer. The purity of the substances and the progress of the reactions were monitored by TLC on silica gel.

2.5. Characterisation

The crystalline phase identification and phase purity determination of the calcined samples of HPWA/MCM-41 were carried out by XRD (Philips, Holland) using nickel filtered Cu Kα radiation (λ = 1.5406 Å). The samples were scanned from 1° to 40° (2θ) angle in steps of 0.02°, with a count of 5 s at each point. Slits were used in this work, in order to protect the detector from the high energy of the incident and diffracted beam. ASAP-2010 volumetric adsorption analyzer manufactured by the Micromeritics Corporation (Norcross, GA) was used to determine the specific surface area of the catalysts at liquid nitrogen temperature. Before the measurement, each sample was degassed at 623 K at 10^{-5} Torr overnight in an outgassing station of the adsorption apparatus. The full adsorption–desorption isotherms were obtained using the BET method at various relative pressures; the pore size distribution and wall thickness were calculated from the nitrogen adsorption–desorption isotherms using the BJH algorithm (ASAP-2010 built-in software from Micromeritics). Mid-infrared spectra of MCM-41 molecular sieves were recorded on a Nicolet (Avatar 360) instrument using a KBr pellet technique. About 4 mg of the sample was ground with 200 mg of spectral grade KBr to form a mixture, which was then made into a pellet using a hydraulic press. This pellet was used for recording the infrared spectra in the range of 4000–400 cm^{-1}. The acidity of all the catalytic systems was analyzed by pyridine adsorption followed by FT-IR spectroscopy in the absorbance mode on a Nicolet 800 (AVATAR) FT-IR spectrometer, fully controlled by the OMNIC software, and an all-glass high-vacuum system. ^{31}P MAS NMR spectra were measured at room temperature on a Bruker Avance DSX 400 FT-NMR spectrometer in the frequency range of 10 kHz, pulse duration 12 μs, delay between pulses 30 s. The instrument was equipped with a Doty Scientific 5 mm Solids MAS Probe, as described elsewhere and the external reference 1% H_3PO_4 in D_2O was used. The accuracy of the chemical shift determination was within ±0.4 ppm. The tungsten content in supported catalysts was recorded using ICP-AES Optima 5300 DV (PerkinElmer) instrument. The dispersion of the HPWA was determined by means of TEM measurements. TEM was performed using a Philips CM 30 ST electron microscope operated at 300 kV. Samples for TEM were prepared by placing droplets of a suspension of the sample in methanol on a polymer microgrid supported on a Cu grid.
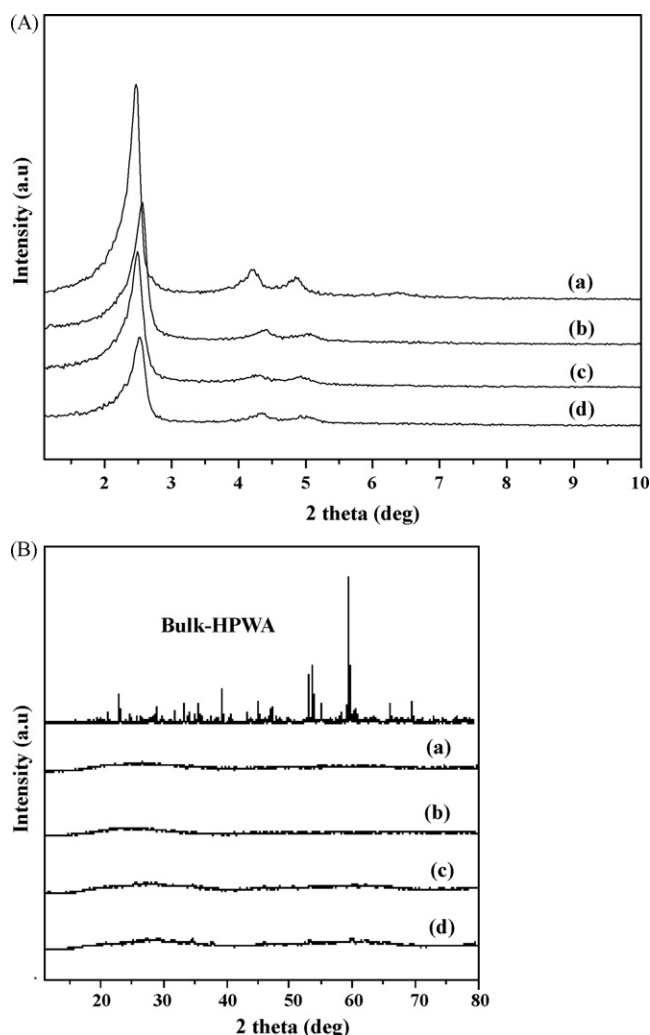
(A)

(B)

Bulk-HPWA

Fig. 1. (A) X-ray diffraction patterns of MCM-41 molecular sieves [low angle (2θ: 1–10°)]: (a) Si-MCM-41, (b) 10% HPWA/Si-MCM-41, (c) 20% HPWA/Si-MCM-41, and (d) 30% HPWA/Si-MCM-41. (B) X-ray diffraction patterns of MCM-41 molecular sieves [high angle (2θ: 10–80°)]: (a) Si-MCM-41, (b) 10% HPWA/Si-MCM-41, (c) 20% HPWA/Si-MCM-41, and (d) 30% HPWA/Si-MCM-41 and bulk HPWA.

3. Results and discussion

3.1. Characterisation of HPWA/MCM-41 catalysts

3.1.1. XRD

The XRD diffraction patterns for calcined HPWA/MCM-41 and Si-MCM-41 materials are shown in Fig. 1 and the data are presented in Table 1. The patterns illustrate the characteristics of a typical mesoporous MCM-41 structure since the materials show the diffraction peaks below 10° (2θ) which correspond to the planes
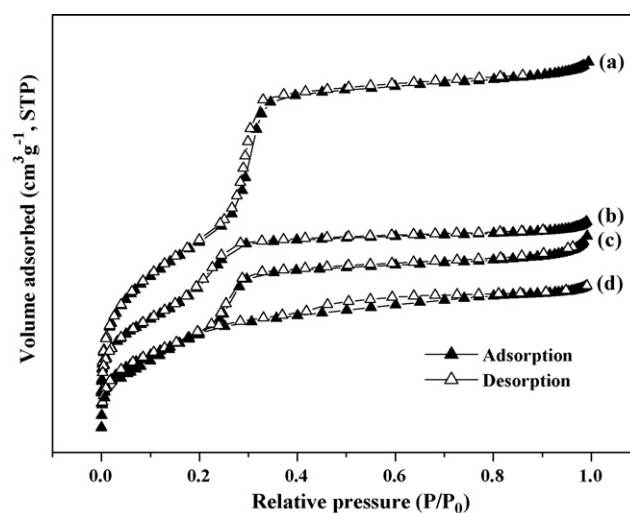
Fig. 2. Nitrogen adsorption–desorption isotherms of the catalysts: (a) Si-MCM-41, (b) 10% HPWA/Si-MCM-41, (c) 20% HPWA/Si-MCM-41, and (d) 30% HPWA/Si-MCM-41.

(1 0 0), (1 1 0), (2 0 0) and (2 1 0). The XRD of HPWA/MCM-41 in particular shows the effect of the PW loading on the XRD of MCM-41 samples. HPWA has a striking effect on the width and intensity of the main reflection at high d_{100} spacing and this line becomes broader and weaker as the loading increases and the peak height is inversely proportional to the amount of loaded HPW. This suggests that the long-range order of Si-MCM-41 is decreased noticeably by the presence of HPWA. Bulk HPWA crystal phase does not appear in the HPWA supported Si-MCM-41 material, indicating that HPWA is finely dispersed on the MCM-41 support.

3.1.2. Nitrogen adsorption isotherms

The data of BET surface area, pore size and pore volume of calcined HPWA/MCM-41 and Si-MCM-41 are presented in Table 1. The BET surface area and the pore volume of the HPWA/Si-MCM-41 samples decrease from 765 to 561 m^2/g and from 0.479 to 0.338 cc/g, respectively. However, the pore size distribution of the mesoporous part is centered at about 2.75–2.68 nm. The pore size of the HPWA/Si-MCM-41 samples is smaller than that of Si-MCM-41. This shows that HPWA has been dispersed on the surface of the mesopores of Si-MCM-41, which is due to the blockage of particles in one-dimensional mesopores of Si-MCM-41 by small aggregates of HPWA. Fig. 2 shows N$_2$ adsorption–desorption isotherms of Si-MCM-41 and all the HPW/Si-MCM-41 samples. It can be seen that MCM-41 presents the highest surface area and pore volume, with all pores being in the mesopore range. With increasing PW loading, a reduction in the pore volume and a prominent density of the pore size distribution are observed as shown in Fig. 3.

Table 1
Physicochemical characterisation of HPWA/MCM-41 type materials.

Catalysts	XRD		BET surface area[b] (m^2/g)	Pore size[b] BJH$_{Ads}$ (nm)	Pore volume[b] BJH$_{Ads}$ (cc/g)	ICP[c] W (wt.%)
	d spacing[a] (Å)	a_o[a] (nm)				
Si-MCM-41 (∞)	39.44	4.55	970	2.983	0.754	–
10% HPWA/Si-MCM-41	37.25	4.30	765	2.776	0.479	6.9
20% HPWA/Si-MCM-41	36.89	4.25	660	2.752	0.402	14.1
30% HPWA/Si-MCM-41	36.32	4.19	561	2.678	0.338	21.2

[a] Values obtained from XRD studies.

[b] Values obtained from N$_2$-adsorption results.
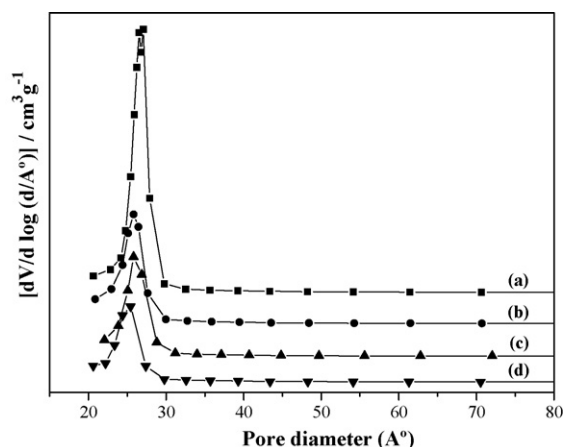
[c] Measured by ICP-AES techniques.

Fig. 3. Pore size distribution of the catalysts: (a) Si-MCM-41, (b) 10% HPWA/Si-MCM-41, (c) 20% HPWA/Si-MCM-41, (d) 30% HPWA/Si-MCM-41.

3.1.3. FT-IR spectroscopy

The FT-IR spectra of the HPWA loaded MCM-41 samples and bulk HPWA are given in Fig. 4. In Fig. 4(a), a broad band around 3430 cm^{-1} is due to the OH stretching vibration of MCM-41 which could be associated to Si–OH and water vibration and another broad band around 1300–1000 cm^{-1} corresponds to the asymmetric stretching mode of Si–O–Si. The bands at 800 and 461 cm^{-1} are assigned to symmetric stretching vibration and bending vibration of the rocking mode of Si–O–Si, respectively. A band at 967 cm^{-1} is due to symmetric stretching vibration of Si–OH. Fig. 4(b) of bulk HPWA with a Keggin structure shows four strong bands at 1084 cm^{-1} (P–O), 983 cm^{-1} (W=O), 895 cm^{-1}, and 801 cm^{-1} (W–O–W), and one weak band at 524 cm^{-1} (W–O–P) [39]. The framework bands of Si-MCM-41 as mentioned for Fig. 4(a) easily overlap with that of HPWA. None of the HPWA bands were observed for 10% HPWA loading except an intense band at 801 cm^{-1}. For 20% and 30% HPWA loadings, two bands at 983 and 895 cm^{-1} became visible. These peaks became more evident with an increase in the HPW loading, due to greater number of oscillators. There was no shift of W=O band occurring after impregnation, as shown in Fig. 4(c–e). It is suggested that HPWA is still intact, after supported on MCM-41.
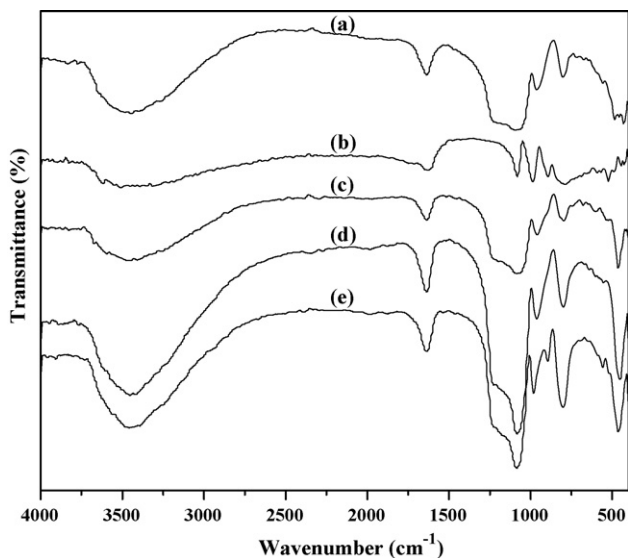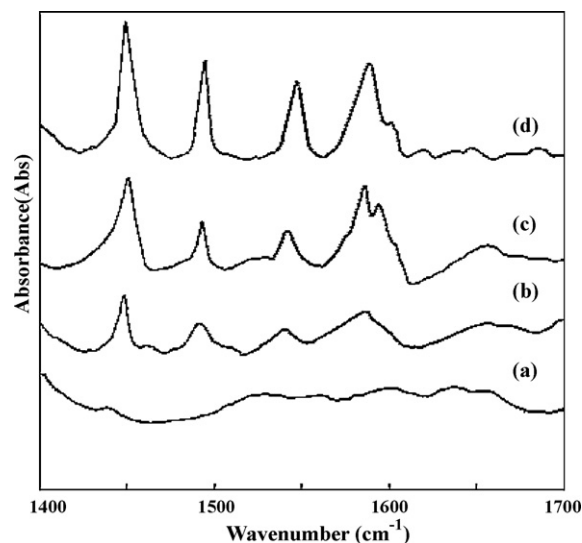

Fig. 5. Pyridine-adsorption FT-IR spectra of the catalysts: (a) Si-MCM-41, (b) 10% HPWA/Si-MCM-41, (c) 20% HPWA/Si-MCM-41 and (c) 30% HPWA/Si-MCM-41.
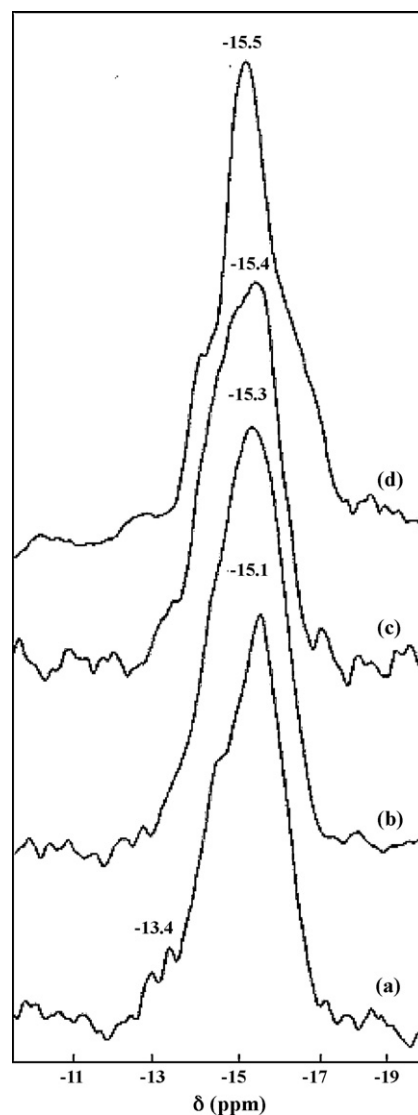

Fig. 4. FT-IR spectra of the catalysts: (a) Si-MCM-41, (b) bulk HPWA, (c) 10% HPWA/Si-MCM-41, (d) 20% HPWA/Si-MCM-41 and (e) 30% HPWA/Si-MCM-41.

Fig. 6. ^{31}P MAS NMR spectra of the catalysts: (a) 10% HPWA/Si-MCM-41, (b) 20% HPWA/Si-MCM-41, (c) 30% HPWA/Si-MCM-41 and (d) bulk HPWA.
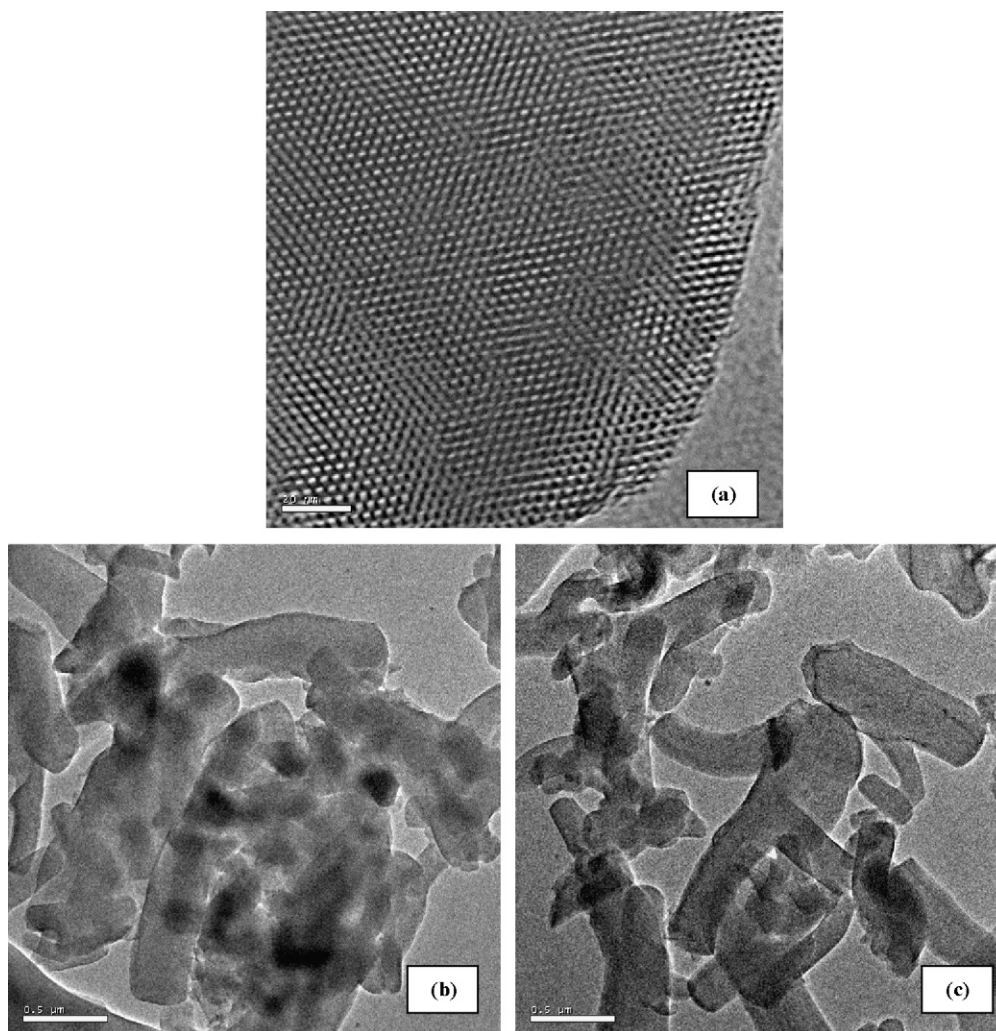
Fig. 7. TEM images of MCM-41 molecular sieves: (a) Si-MCM-41, (b) 20% HPWA/Si-MCM-41, and (c) 30% HPWA/Si-MCM-41.

3.1.4. Pyridine adsorbed FT-IR spectroscopy

Pyridine adsorbed FT-IR spectra of HPWA/MCM-41 samples containing adsorbed pyridine are presented in Fig. 5. A more intense peak that appears at 1445 cm^{-1} is due to the pyridine adsorbed on Lewis acid sites, a less intense peak at 1545 cm^{-1} is due to adsorption on Bronsted acid sites and a peak around 1493 cm^{-1} are due to both Bronsted and Lewis acid sites. Bronsted acid sites are due to the presence of small clusters of heteropoly acid, while the Lewis acid sites might be due to the interaction of heteropoly acid with framework SiO$_2$. In HPWA/MCM-41 samples, the acidity increases gradually with increasing HPWA loading from 10 to 30 wt.%. At higher loadings, interactions between HPWA and the MCM-41 surface may have a negative effect on the activity of these materials, as they appear to be responsible for severe distortion of the structural wall [39,40]. This steady rise in the acidity of the materials with higher HPWA loadings suggest that there is no collapse of the structure wall in spite of this high loading. This was further confirmed by XRD (Fig. 1).

3.1.5. ^{31}P MAS NMR

^{31}P MAS NMR spectra of HPW/MCM-41 samples with different acid loadings revealed that the Keggin structure of the catalyst was unaffected after loading HPWA on Si-MCM-41 support and remains intact, illustrating a peak around −15.1, −15.3 and −15.4 ppm for 10, 20 and 30 wt.% HPWA loading on Si-MCM-41, respectively compared to that obtained for bulk HPWA around −15.5 ppm as in Fig. 6. The observations predicts that there is a strong resonance at −15 ppm corresponding to the tetrahedral coordination of PO$_4$ in the Keggin unit [29].
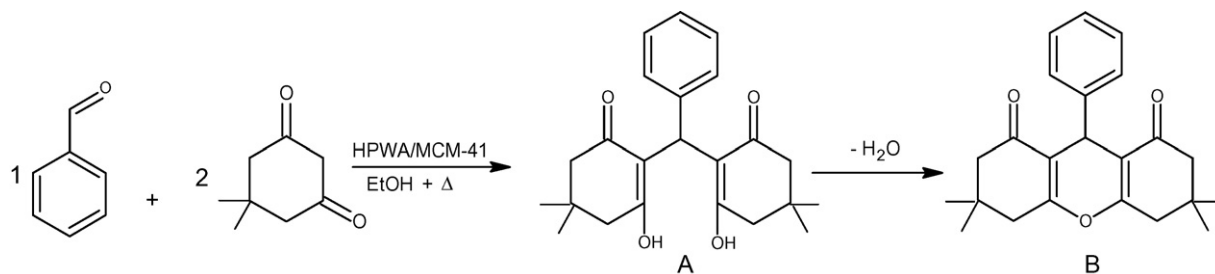
3.1.6. TEM analysis

The morphology of the Si-MCM-41 and supported catalysts was consistent with TEM results (Fig. 7). TEM images depicts a honey-comb structure of the host material, whereas 20% and 30% HPWA containing Si-MCM-41 shows the uniform dispersion of HPWA on the host, which can be distinguished as dark dots. The existence of large PW crystals on the MCM-41 and a fine dispersion is noticed.

3.2. Catalytic studies

3.2.1. Synthesis of 1,8-dioxo-octahydroxanthenes (xanthenediones) from dimedone and aromatic aldehydes through addition and cyclo-dehydration

The synthesis of xanthenediones was performed by taking a mixture of stoichiometric amount of dimedone (2 mol), aromatic aldehyde (1 mol) along with calculated amount of catalyst in a selected solvent at appropriate temperatures under liquid phase conditions. The reaction involves two steps to yield the expected xanthenediones; the first step is the addition step to form an

intermediate A and the second being the (Knoevenagel type) condensation step with the elimination of a water molecule to form the product B.

decreased (2:1 = 85% and 3:1 = 94%). This may be due to the availability of the reactant (dimedone) near the Bronsted acid sites as

3.2.2. Effect of substituents of benzaldehyde on product yield

Different substituted xanthenediones were prepared from various aromatic aldehydes and 5,5-dimethyl-1,3-cyclohexanedione. About 10 substituted xanthenedione derivatives were obtained as shown in Table 2 such as: Entry [a] 3,3,6,6-tetramethyl-9-phenyl-1,2,3,4,5,6,7,8-octahydro-xanthene-1,8-dione, Entry [b] 3,3,6,6-tetramethyl-9-(4′-nitrophenyl)-1,2,3,4,5,6,7,8-octahydro-xanthene-1,8-dione, Entry [c] 3,3,6,6-tetramethyl-9-(3′-nitrophenyl)-1,2,3,4,5,6,7,8-octahydro-xanthene-1,8-dione, Entry [d] 3,3,6,6-tetramethyl-9-(2′-chlorophenyl)-1,2,3,4,5,6,7,8-octahydro-xanthene-1,8-dione, Entry [e] 3,3,6,6-tetramethyl-9-(4′-chlorophenyl)-1,2,3,4,5,6,7,8-octahydro-xanthene-1,8-dione, Entry [f] 3,3,6,6-tetramethyl-9-(4′-methoxyphenyl)-1,2,3,4,5,6,7,8-octahydro-xanthene-1,8-dione, Entry [g] 3,3,6,6-tetramethyl-9-(4′-hydroxy-3′-methoxyphenyl)-1,2,3,4,5,6,7,8-octahydro-xanthene-1,8-dione, Entry [h] 3,3,6,6-tetramethyl-9-(2′-hydroxyphenyl)-1,2,3,4,5,6,7,8-octahydro-xanthene-1,8-dione, Entry [i] 3,3,6,6-tetramethyl-9-(4′-hydroxyphenyl)-1,2,3,4,5,6,7,8-octahydro-xanthene-1,8-dione and Entry [j] 3,3,6,6-tetramethyl-9-(2′-methoxyphenyl)-1,2,3,4,5,6,7,8-octahydro-xanthene-1,8-dione.

The presence of electron-donating (nitro or halide group) or electron-withdrawing groups (alkoxy or hydroxyl group) in the aromatic ring of the aldehydes did not have much effect on the reaction such that to afford respective products with high yields. But para-substituted aldehydes gave good results compared to the ortho-substituents. There is more steric hindrance for the ortho substituted aldehydes (o-OCH$_3$, -OH, -Cl, -NO$_2$) on the product formation than the para-substituted (p-OCH$_3$, -OH, -Cl, -NO$_2$) aldehydes.

3.2.3. Effect of different solvents on product yield

The condensation reaction to yield xanthenediones was tested with different solvents such as ethanol, methanol, acetonitrile, ethyl acetate and toluene. The order of various solvents over product yield is as follows: ethanol > acetonitrile > ethyl acetate > methanol > toluene, as shown in Table 3. Since the more polar nature of the solvent is concerned with the active centres of the catalyst to drive the products at its surface, ethanol and acetonitrile were found to be more suitable for the reaction to yield pure xanthenediones. The less polar solvents like toluene showed low product yield and there was no reaction when solvents like DMSO and DMF are used; due to their nature of adsorption on catalyst surface or reactants it is suggested that they retard the condensation of the intermediates.

3.2.4. Effect of molar ratio

In general, 2 mol dimedone and 1 mol aromatic aldehyde (2:1) is the basic stoichiometry to yield xanthenediones. The ratio of dimedone to aromatic aldehyde was altered to check the influence of molar ratio such as 2:1, 3:1, 4:1 and 5:1. The yield was found to increase with increasing molar ratio up to mole ratio 3:1 and then

they promote the dehydration mechanism. One can suggest that the promotion of eliminating the water molecules decreases, once the pores of the catalyst get blocked by the product precipitation. The high surface area of the catalysts and higher acidity prevents such diffusion problems as the bulky molecules pass through the pores with ease.

3.2.5. Effect of catalyst

The reaction of dimedone and aromatic aldehyde was performed over various catalysts to test their catalytic activity individually. All the catalysts were compared to support the activity based on the product yield, recovery and reusability. The activity of the catalysts used were in the order; HPWA/MCM-41(20 wt.%) > HPWA/MCM-41(30 wt.%) > H$_3$PW$_{12}$O$_{40}$·nH$_2$O > HPWA/MCM-41(10 wt.%) > 20% HPWA/SiO$_2$ > HM (12) > Hβ (8) > Al-MCM-41 (50), as shown in Table 4. The prominent efficient catalyst was HPWA/MCM-41 (20 wt.%) for all the substituted xanthenediones.

When compared with the catalysts above, all type of zeolites gave the low xanthenedione yield, which is attributed mainly to the small pore size and surface area leading to the diffusion problems of reactants and products together with lower acidity. The activity of 20 wt.% HPWA/MCM-41 is significantly higher than that of the 30 wt.% HPWA/MCM-41. The low HPWA content of 10 wt.% loading resulting in the low activity among these catalysts. The partial impasse of one-dimensional mesopores of Si-MCM-41 due to the observed deliberate decrease in the pore size with increasing HPWA loading and the hasty decrease in the BET surface area and the pore volume at higher loading of HPWA are the grounds for the slight lower activity of 30 wt.% HPWA/MCM-41 compared to that of 20 wt.% HPWA/MCM-41. The product yield was very low for Al/MCM-41 and this may be due to the lower acidity of the catalyst rendering the product formation. The HPWA supported silica gel catalysts showed low activity compared to MCM-41 catalysts. Of all the catalysts, supported HPWA catalysts possessing more acidity, wide porosity and large surface area were effective for the synthesis of xanthenediones. Turnover number (TON) for 20 wt.% HPWA/MCM-41 catalyst to yield the product 3,3,6,6-tetramethyl-9-phenyl-1,2,3,4,5,6,7,8-octahydro-xanthene-1,8-dione (Entry [a]) are presented in Table 5. The turnover of the reaction was studied using 0.25 g of 20 wt.% HPWA/Si-MCM-41 with varying the reactant concentrations under the reaction conditions; temperature = 90 °C; time = 5 h; feed ratio = 3:1 (dimedone/benzaldehyde); solvent = ethanol. It was observed that the turnover number increased from 18.8 to 184 and thereafter decreased to 153. From this observation it can be concluded that 20 wt.% HPWA/Si-MCM-41 is efficient for the synthesis of biologically active xanthenedione derivatives.

3.2.6. Structural determination of isolated products

Primary elucidation of the structures for all the isolated products was done by FT-IR spectra as in Fig. 8. For Entry [a]—Table 3;

Table 2
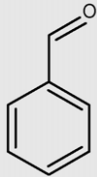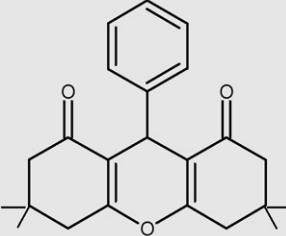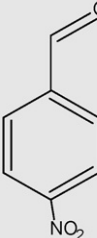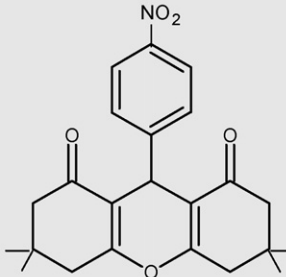Synthesis of xanthenediones over various % of HPWA loaded Si-MCM-41.
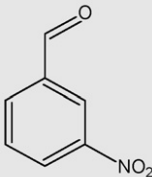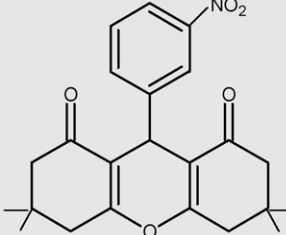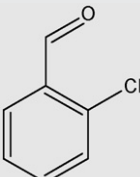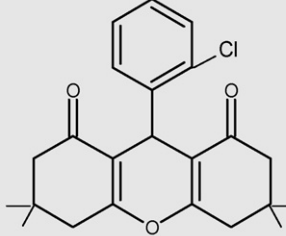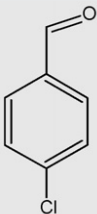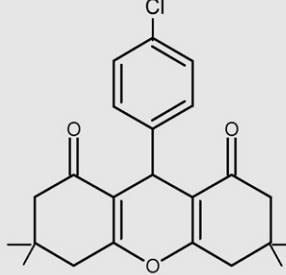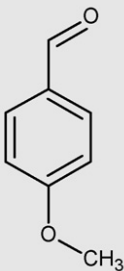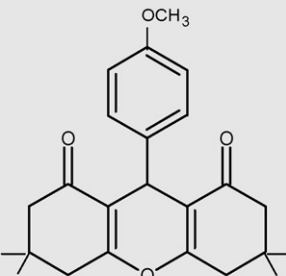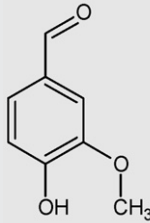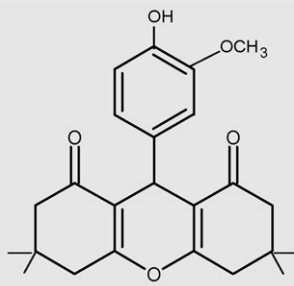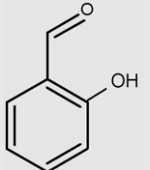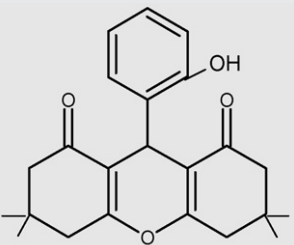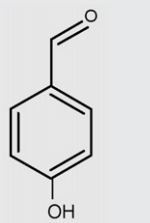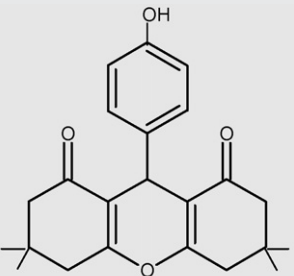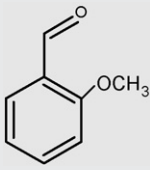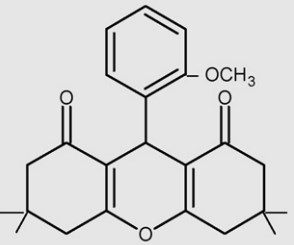
Entry	Aldehyde	Compound	Isolated yield (%)	
			20 wt.% HPWA/MCM-41	30 wt.% HPWA/MCM-41
[a]			94	85
[b]			87	82
[c]			86	81
[d]			90	83
[e]			93	84
[f]			89	81

Table 2 (*Continued*)

Entry	Aldehyde	Compound	Isolated yield (%)	
			20 wt.% HPWA/MCM-41	30 wt.% HPWA/MCM-41
[g]			87	74
[h]			89	76
[i]			93	81
[j]			81	75

Reaction conditions: temperature = 90 °C; reaction vessel = 25 ml; time = 5 h; solvent = ethanol (5 ml); mole ratio = 3:1 (dimedone/benzaldehyde); catalyst = 20 wt.% HPWA/MCM-41 and 30 wt.% HPWA/MCM-41; Wt. of the catalyst = 0.25 g.

Table 3
Effect of various solvents on the condensation of dimedone with benzaldehyde over 20 wt.% HPWA/MCM-41.

Sl. no.	Solvents	Yield of xanthenedione (%)
1	Ethanol	94
2	Acetonitrile	82
3	Ethyl acetate	71
4	Methanol	70
5	Toluene	64

Reaction conditions: temperature = 90 °C; mole ratio = 3:1 (dimedone/benzaldehyde); catalyst = 20 wt.% HPWA/MCM-41; time = 5 h; Wt. of the catalyst = 0.25 g.

Table 4
Effect of various catalysts on condensation of dimedone with benzaldehyde.

Sl. no.	Catalysts	Isolated yield (%)
1	10% HPWA/MCM-41	71
2	20% HPWA/MCM-41	94
3	30% HPWA/MCM-41	85
4	10% HPWA/SiO$_2$	47
5	20% HPWA/SiO$_2$	59
6	30% HPWA/SiO$_2$	58
7	H$_3$PW$_{12}$O$_{40} \cdot n$H$_2$O	75
8	HM (12)	58
9	Hβ (8)	54
10	Al-MCM-41	50
11	Without catalyst	7

Reaction conditions: temperature = 90 °C; time = 5 h; feed ratio = 3:1 (dimedone/benzaldehyde); catalyst loading = 0.25 g; solvent = ethanol.

Table 5
Turnover number for 20 wt.% HPWA/Si-MCM-41 over the condensation of dimedone with benzaldehyde (Entry [a]).

Acid amount of catalyst (mmol)	Benzaldehyde (mmol)	Isolated yield of xanthenedione (%)	TON[a]
0.05	1	94	18.8
0.05	5	93	93.0
0.05	10	92	184.0
0.05	15	51	153.0

[a] TON—turnover number: number of moles of product per mole of acid amount of catalyst. Reaction conditions: temperature = 90 °C; time = 5 h; feed ratio = 3:1 (dimedone/benzaldehyde); catalyst (20 wt.% HPWA/Si-MCM-41) = 0.25 g; solvent = ethanol.
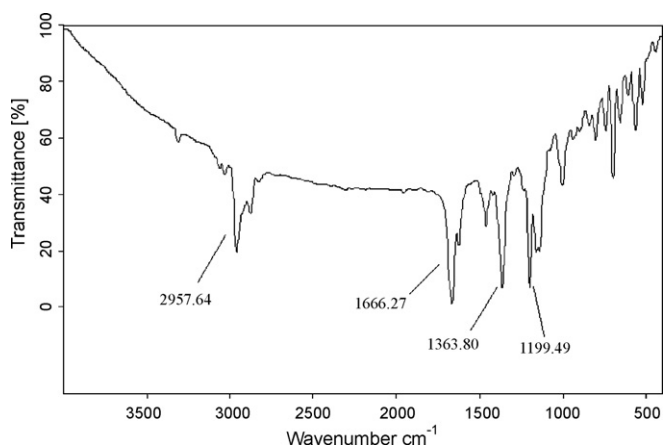

Fig. 8. FT-IR spectrum of the compound [Table 3, entry [a]]: IR (KBr); 2957.64, 1666.27, 1363.80, and 1199.49 cm^{-1}.

a medium band obtained at 2957 cm^{-1} represents the presence of alkanes (4 CH$_3$ groups), a strong band at 1666 cm^{-1} represents the presence of general carbonyl groups (C=O stretching), a medium band at 1364 cm^{-1} for alkanes (C–H bending), a strong band at 1199 cm^{-1} confirms the presence of ether (C–O stretching). The determination of structures for the products was further confirmed by ^{1}H NMR spectra. A singlet obtained at 4.75 (s, 1H, CH) (as in Fig. 9) confirms the formation of product, 3,3,6,6-tetramethyl-9-phenyl-1,2,3,4,5,6,7,8-octahydro-xanthene-1,8-dione.
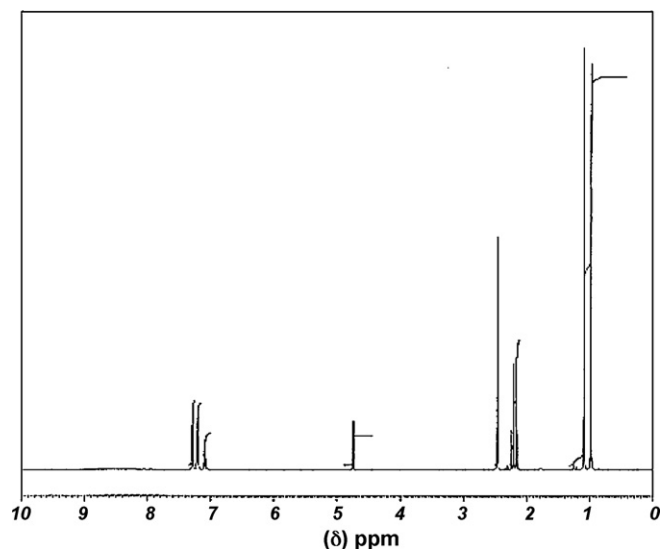

Fig. 9. ^{1}H NMR (CDCl$_3$, 500 MHz) spectrum of the compound [Table 3, entry [a]]: 0.99 (s, 6H, 2CH$_3$), 1.1 (s, 6H, 2CH$_3$), 2.2 (dd, 4H, J = 1.6, 4.0 Hz, 2CH$_2$), 2.5 (s, 4H, 2CH$_2$), 4.75 (s, 1H, CH), 7.1 (m, 2H, ArH), 7.2 (m, 3H, ArH).

Table 6
Recyclability of supported catalysts (20 wt.% HPWA/MCM-41).

Cycles	W^a (wt.%)	W^b (wt.%)	Isolated yield of xanthenedione^b (%)
Fresh	14.1	–	94
1	11.5	2.5	89
2	10.9	0.5	86
3	10.7	0.15	84

[a] W content in 20 wt.% HPWA/MCM-41 obtained from ICP-AES data.
[b] W content in reaction solvent (ethanol) after each cycles obtained from ICP-AES data.

Table 7
Reusability of 20 wt.% HPWA/MCM-41 catalysts.

Cycles	Isolated yield of xanthenedione^a (%)	Isolated yield of xanthenedione^b (%)
Fresh	94	82
1	89	72
2	86	69
3	84	67

[a] Yield obtained for product (using ethanol as solvent).
[b] Yield obtained for product (using acetonitrile as solvent).

3.2.7. Reusability of the catalysts and the leaching effect

The supported HPWA catalysts were collected by filtration from the solution and washed with acetone and dried to give the material. Leaching of HPWA in 20% HPWA/MCM-41 catalysts was studied by ICP-AES analysis in terms of tungsten percentage. The loading amount of H$_3$PW$_{12}$O$_{40}$ in the supported catalysts was measured in terms of tungsten percentage as obtained from ICP-AES results. The W% of first, second and third cycles for 20 wt.% catalysts after the reaction were 11.5, 10.9 and 10.7, respectively. The W% in the catalyst and that in the solution are presented in Table 6. There was significant loss of tungsten for the first cycle when ethanol is used as solvent but the loss diminished for later cycles. From the catalytic runs observed, the product yield was gradually decreased for the recycle use as shown in Table 7.

4. Conclusion

The present work involves the target synthesis of biologically active xanthenediones over supported HPWA catalysts. The Bronsted acidic nature of the supported HPW materials determines the effective condensation pathway in order to give good product yields and the acidity of the supported HPWA increases with loading. There is a decrease in pore size and pore volume at higher loading of HPWA. Supported HPWA catalysts give good results compared to bulk HPWA. Regarding the nature of the aldehydes, the *para*-substituted aldehydes give better yields than the *ortho*-substituents since the steric hindrance of the later restricts the product formation. The practical simplicity of the procedures, short reaction times, recoverability and reusability attracts attention to the applications of the materials.

References

[1] K. Chibale, M. Visser, D.V. Schalkwyk, P.J. Smith, A. Saravanamuthu, A.H. Fairlamb, Tetrahedron 59 (13) (2003) 2289–2296.
[2] S. Hatakeyma, N. Ochi, H. Numata, S. Takano, J. Chem. Soc., Chem. Commun. (1988) 1202.
[3] G.M. Cingolant, M. Pigini, J. Med. Chem. 12 (1988) 531.
[4] C.N. O'Callaghan, T.B.H. McMurry, J. Chem. Res. Synop. 214 (1995); C.N. O'Callaghan, T.B.H. McMurry, J. Chem. Res. (1995) 1448, Miniprint, and refs. cited therein.
[5] E.S.H. El Ashry, L.F. Awada, E.S.I. Ibrahim, O.K. Bdeewy, Arkivoc (ii) (2006) 178–186.
[6] J. Kuthan, P. Sebek, S. Bohm, Advances in Heterocyclic Chemistry, vol. 62, Academic Press, Inc., New York, 1995, p. 19.
[7] N. Rashed, M. Sayed, E.S.H. El Ashry, J. Chin. Chem. Soc. 40 (1993) 189.

[8] H. Abdel Hamid, A. Mousaad, M. Sayed, E.S.H. El Ashry, Org. Prep. Proced. Int. 25 (1993) 596.
[9] N. Rashed, E.S.H. El Ashry, Alex, J. Pharm. Sci. 7 (1993) 137.
[10] E.C. Horning, M.G. Horning, J. Org. Chem. 11 (1946) 95–102.
[11] D.Q. Shi, Q.Y. Zhuang, Chin. J. Org. Chem. 23 (2003) 694.
[12] D.Q. Shi, Y.C. Wang, Z. Lu, G. Dai, Synth. Commun. 30 (2000) 713.
[13] X. Fan, X. Hu, X. Zhang, J. Wang, Can. J. Chem. 83 (2005) 16–20.
[14] G. Song, B. Wang, H. Luo, L. Yang, Catal. Commn. 8 (2007) 673–676.
[15] B. Das, P. Thirupathi, I. Mahender, V.S. Reddy, Y.K. Rao, J. Mol. Catal. A: Chem. 247 (2006) 233–239.
[16] X.S. Fan, Y. Zhen, X.Y. Zhang, X.Y. Hu, J.J. Wang, Chin. Chem. Lett. 16 (7) (2005) 897–899.
[17] T.S. Jin, J.S. Zhang, J.C. Xiao, A.Q. Wang, T.S. Li, Synth. Lett. 5 (2004) 866–870.
[18] M.M. Amini, M. Seyyedhamzeh, A. Bazgir, Appl. Catal. A 323 (2007) 242–245.
[19] M.M. Heravi, K. Bakhtiari, Z. Daroogheha, F.F. Bamoharram, J. Mol. Catal. A 273 (2007) 99–101.
[20] H.N. Karade, M. Sathe, M.P. Kaushik, Arkivoc (xiii) (2007) 252–258.
[21] K.M. Reddy, C. Song, Catal. Today 31 (1996) 137–144.
[22] A.S. Farhanullah, P.R. Maulik, V.J. Rama, Tetrahedron Lett. 45 (26) (2004) 5099–5102.
[23] G. Song, B. Wang, G. Wang, R. Kang, T. Yang, L. Yang, Synth. Commun. 35 (2005) 1051–1057.
[24] E. Armengol, A. Corma, H. Garcia, M.T. Navarro, J. Chem. Soc., Chem. Commun. 5 (1995) 519–520.
[25] K. Okumura, K. Nishigaki, M. Niwa, Microporous Mesoporous Mater. 44–45 (2001) 509–516.
[26] M.V. Landau, E. Dafa, M.L. Kaliya, T. Sen, M. Herskowitz, Microporous Mesoporous Mater. 49 (2001) 65–81.
[27] M.J. Climent, A. Corma, S. Iborra, M.C. Navarro, J. Primo, J. Catal. 161 (1996) 783–789.
[28] L.X. Dai, K. Koyama, T. Tatsumi, Catal. Lett. 53 (1998) 211–214.
[29] V.R. Choudhary, V.H. Tillu, V.S. Narkhede, H.B. Borate, R.D. Wakharkar, Catal. Commn. 4 (9) (2003) 449–453.
[30] A.L. Villade, P.E. Alarcon, C.M. de Correa, Chem. Commun. (2002) 2654.
[31] I.V. Kozhevnikov, Catal. Rev. Sci. Eng. 37 (1995) 311.
[32] M.J. Janik, R.J. Davis, M. Neurock, J. Catal. 244 (2006) 65–77.
[33] W. Chu, X. Yang, Y. Shan, X. Ye, Y. Wu, Catal. Lett. 42 (1996) 201–208.
[34] I.V. Kozhevnikov, A. Sinnema, R.J.J. Janse, K. Pamin, H. van Bekkum, Catal. Lett. 30 (1995) 241–252.
[35] Y. Izumi, H.R.K. Urabe, J. Catal. 84 (1983) 402–409.
[36] S. Ajaikumar, A. Pandurangan, J. Mol. Catal. 286 (2008) 21–30.
[37] T. Blasco, A. Corma, A. Martinez, P.M. Escolano, J. Catal. 177 (1998) 306–313.
[38] J.S. Beck, J.C. Vartuli, W.J. Roth, M.E. Leonowicz, C.T. Kresge, K.D. Schmitt, C.T.-W. Chu, D.H. Olson, E.W. Sheppard, S.B. McCullen, J.B. Higgins, J.L. Schlenker, J. Am. Chem. Soc. 114 (1992) 10834–10843.
[39] Q.-H. Xia, K. Hidajat, S. Kawi, J. Catal. 205 (2002) 318–331.
[40] Q.-H. Xia, K. Hidajat, S. Kawi, J. Catal. 209 (2002) 433–444.